Quantum statistics of three modes coupled oscillators

1998 J. Phys. A: Math. Gen. 31 3117

(http://iopscience.iop.org/0305-4470/31/14/003)

J. Phys. A: Math. Gen. **31** (1998) 3117–3139. Printed in the UK PII: S0305-4470(98)87984-5

Quantum statistics of three modes coupled oscillators

M Sebawe Abdalla†, M M A Ahmed‡ and S Al-Homidan§

† Mathematics Department, College of Science, King Saud University, PO Box 2455, Riyadh 11451, Saudi Arabia

‡ Mathematics Department, Faculty of Science, Al-Azhar University, Nasr City, Cairo, Egypt

§ Mathematical Sciences Department, College of Science, King Fahd University of Petroleum and Minerals, PO Box 119, Dhahran 31261, Saudi Arabia

Received 29 September 1997, in final form 17 December 1997

Abstract. From a quantum optics point of view the problem of three modes time-dependent coupled oscillators is considered. The connection related to the directional coupler is given, and the solution in the Heisenberg picture is obtained. The Glauber second-order correlation function has been used to discuss the bunching and antibunching. The phenomena of squeezing as well as the quasiprobability distribution functions (Wigner function and Q-function) are examined.

1. Introduction

The problem of three modes interaction can be regarded as one of the most fundamental problems to the field of quantum optics. In the optical regime there are two different types of these interactions; one is called a frequency converter, while the second is known as a parametric amplifier [1, 2]. The parametric frequency conversion occurs in a number of well known phenomena. These include the production of anti-Stokes radiation in Raman and Brillouin scattering and the up conversion of light signals in nonlinear media [3–5]. Meanwhile one can see the frequency splitting of light beams is an example of parametric amplification in which both of the coupled modes are electromagnetic. The most familiar form of the parametric amplifier is designed to amplify an oscillating signal by means of particular coupling of the mode in which it appears to a second mode of oscillation, the idler mode. The coupling parameter is made to oscillate with time in a way which gives rise to a steady increase of the energy in both the signal and idler modes. It is worthwhile referring to the coherent Raman effect, where the presence of a monochromatic light wave in a Raman active medium gives rise to parametric coupling between an optical vibrational mode and a mode of the radiation field which represents the scattered Stokes. The same situation may be found in the case of Brillouin scattering, where the vibrational mode oscillates at an acoustic, rather than an optical, frequency. We may refer to electrical engineering applications, where microwave versions of the parametric amplifier and frequency converter have been used. For example we can find at optical frequencies, the spontaneous emission of quanta, which is not predicted by classical theory, is an important contribution. Finally, refer to the recent experiment by Geordiades *et al* [6], where the squeezed light is generated by non-degenerate parametric down conversion in order to excite a two-photon transition in atomic caesium. Thus, a theoretical description of the amplification and frequency conversion of light must take quantum effects into account. In the field of quantum optics it is well known that the susceptibility $\chi^{(2)}$ leads to a cubic nonlinearity which is responsible for the three-wave mixing processes in parametric devices, as well as second harmonic and sub-harmonic generation [7–9]. Therefore one can see the most familiar Hamiltonian which describes the above phenomena in terms of boson operators is the trilinear Hamiltonian [10–13]

$$\frac{H}{\hbar} = \sum_{i=1}^{3} \omega_i a_i^\dagger a_i + \lambda(a_1^\dagger a_2 a_3 + a_1 a_2^\dagger a_3^\dagger) \tag{1.1}$$

where a_i and $a_i^\dagger$ are boson operators of the ith mode with angular frequency ω_i, while λ is nonlinear coupling depends in general on the susceptibility $\chi^{(2)}$. In fact the above Hamiltonian has been considered extensively to describe the non-degenerate three-wave interactions in different phase regimes. For example, the authors of [11] showed that, with an initial Kerr state it is possible to get strongly sub-Poissonian photon statistics in the signal after a short time of interaction, provided the photon numbers do not change in the first order of time. We may also refer to the authors of [12], where they have used the Hamiltonian model; equation (1.1) to describe three boson fields with the decay of Rayleigh mode into the Stokes and vibration (phonon) modes, and discussed the possibility of using the correlation Raman spectroscopy to measure the quantum-statistical properties of the vibration mode. Although there are many attempts to find a solution of the equations of motion in the Heisenberg picture for equation (1.1), however, it is not an easy task to obtain an exact solution in compact and closed form [13]. Therefore, to find an exact solution we can use what is called the parametric approximation, where the strong pump wave (laser mode) is treated as a C-number, and any depletion is neglected while the relatively weak signal and idler can drastically change. Under this approximation the Hamiltonian (1.1) takes the form

$$\frac{H}{\hbar} = \omega_1 a_1^\dagger a_1 + \omega_2 a_2^\dagger a_2 + g_1(a_1^\dagger a_2^\dagger \mathrm{e}^{\mathrm{i}\tilde{\omega}t} + a_1 a_2 \mathrm{e}^{-\mathrm{i}\tilde{\omega}t}) \tag{1.2}$$

where $\tilde{\omega}$ (the frequency pump) is equal to $(\omega_1 + \omega_2)$. The Hamiltonian (1.2) represents the parametric amplifier model. Alternatively we may use a different approach to linearize equation (1.1), that is to treat either the signal or idler mode as a C-number. Thus we have

$$\frac{H}{\hbar} = \omega_1 a_1^\dagger a_1 + \omega_3 a_3^\dagger a_3 + g_2(a_1^\dagger a_3 \mathrm{e}^{\mathrm{i}\bar{\omega}t} + a_1 a_3^\dagger \mathrm{e}^{-\mathrm{i}\bar{\omega}t}) \tag{1.3}$$

where the frequency $\bar{\omega}$ is equal to $(\omega_1 - \omega_3)$, and the Hamiltonian in this case is known as a frequency converter model. The last two equations may be derived by using an alternative method. For example in the quantization of the cavity modes, one finds that the total energy of the field is [1, 14]

$$H_0 = \frac{1}{8\pi}\int_{\text{cavity}} (\in \xi^2 + \mathcal{H}^2)\,\mathrm{d}v \tag{1.4a}$$

where ξ and $\mathcal{H}$ are the electric and magnetic fields respectively, and $\in$ is the dielectric constant. In terms of boson operators we have

$$H_0 = \sum_l \hbar_{\omega_l}(a_l^\dagger a_l + \tfrac{1}{2}) \tag{1.4b}$$

where $\in$ has been taken to be unity.

In order to provide coupling between the various cavity modes, we shall consider that the dielectric constant varies as

$$\in (r, t) = 1 + \Delta \in f(r) \sum_i \cos(\omega_i t + \phi_i) \tag{1.4c}$$

where $f(r)$ is a function of the position vector r, and $\Delta \in \ll 1$ and ϕ_i is an arbitrary pump phase. The total Hamiltonian including the interaction terms becomes, $H = H_0 + H_1$, where H_0 is given by equation (1.4*b*) and H_1 is

$$\frac{H_1}{\hbar} = -\sum_{i,l,m} k_{lm} \cos(\omega_i t + \phi_i)(a_l^\dagger - a_l)(a_m^\dagger - a_m). \tag{1.4d}$$

The coupling coefficients k_{lm} are

$$k_{lm} = \frac{\Delta \in}{16\pi c^2}(\omega_l \omega_m)^{1/2} \int_{\text{cavity}} f(r) u_l(r) u_m(r)\, \mathrm{d}v \tag{1.4e}$$

where $u_l(r)$ are the normal modes satisfying

$$\nabla \wedge \nabla \wedge u_l(r) = \left(\frac{\omega_l}{c}\right)^2 u_l(r). \tag{1.4f}$$

Here it is interesting to refer to the recent work of Garrett *et al* [15], which reported an experimental demonstration of phonon squeezing in a macroscopic system by exciting a crystal KT_aO_3 with an ultrafast pulse of light. The Hamiltonian relevant to their work can be adjusted to be essentially the total of H_0 and H_1. Now if we choose $f(r)$ so that $k_{lm} \neq 0$, this will leave an infinite number of modes coupled. Therefore by a proper choice of the pump frequency ω_i, the interacting modes will be limited to two modes, and then under certain conditions one obtains equations (1.2) and (1.3), see [1, 16–18]. On the other hand we can adjust the pump frequency to obtain the Hamiltonian describing the back-action-evading amplifiers where the Hamiltonian model is constructed by combining parametric amplifiers and parametric frequency converters [19–22]. Furthermore, we may extend the number of modes to be three instead of two. In this case we have

$$\begin{aligned}\frac{H}{\hbar} = \sum_{i=1}^{3} \omega_i a_i^\dagger a_i - \mathrm{i}\lambda_1(a_1 a_2 \mathrm{e}^{\mathrm{i}(\omega_1+\omega_2)t+\mathrm{i}\phi_1} - \text{h.c.}) - \mathrm{i}\lambda_2(a_1 a_3 \mathrm{e}^{\mathrm{i}(\omega_1+\omega_3)t+\mathrm{i}\phi_2} - \text{h.c.}) \\ -\mathrm{i}\lambda_3(a_2 a_3^\dagger \mathrm{e}^{\mathrm{i}(\omega_2-\omega_3)t+\mathrm{i}\phi_3} - \text{h.c.})\end{aligned} \tag{1.5}$$

ω_i and λ_i, $i = 1, 2, 3$ are representing the fields frequencies and the coupling parameters respectively while ϕ_i are arbitrary phases. Equation (1.5) describes the mutual interaction between three modes, the free phonon, Stokes and anti-Stokes. The interaction part represents two different types of interactions. The terms multiplied by λ_1 and λ_2 are parametric amplifications, and the term multiplied by λ_3 is the frequency conversion. In other words, we can say that equation (1.5) describes a two-photon parametric coupling of modes 1 and 2, and 1 and 3 (two photons are simultaneously created or annihilated in both the quantum modes through the interaction with classical pumping mode), and linear interaction of modes 2 and 3. As a special case, if one takes the coupling parameters λ_1 or λ_2 to be zero, then the Hamiltonian (1.5) will reduce to the Hamiltonian model considered in [5, 23], where the statistical properties of photon and phonon fields in Brillouin scattering have been discussed. We may also refer to the authors of [24], where a problem similar to that given in [23] was considered, and pairs of real invariants were obtained. Thus, we may say that the Hamiltonian model (1.5) can be regarded as a generalization to those represented in [5, 23, 24]. The Hamiltonian (1.5) can be transformed to be time independent if we manage to remove the exponential terms from the Hamiltonian. This can be done if one uses the transformation

$$A_j = a_j \exp \mathrm{i}\omega_j t \qquad j = 1, 2, 3. \tag{1.6}$$

In this case equation (1.5) becomes

$$\frac{H}{\hbar} \to \frac{H'}{\hbar} = -\mathrm{i}\lambda_1(A_1A_2 - A_1^\dagger A_2^\dagger) - \mathrm{i}\lambda_2(A_1A_3 - A_1^\dagger A_3^\dagger) - \mathrm{i}\lambda_3(A_3^\dagger A_2 - A_3A_2^\dagger) \tag{1.7}$$

where we have dropped the arbitrary phases ϕ_i.
Note that if we neglect one of the coupling parameters, λ_1 or λ_2, taken into account λ_3, to be zero, then the time-dependent evolution operator for the above Hamiltonian will be identified as a correlated squeeze operator model, which is regarded as the $su(1,1)$-generalized coherent state, see for example (25). On the other hand, if one defines the operators $\hat{A}$, $\hat{B}$ and $\hat{C}$ such that

$$\hat{A} = A_1A_2 - A_1^\dagger A_2^\dagger \tag{1.8a}$$

$$\hat{B} = A_1A_3 - A_1^\dagger A_3^\dagger \tag{1.8b}$$

$$\hat{C} = A_3^\dagger A_2 - A_3A_2^\dagger \tag{1.8c}$$

we find

$$[\hat{A}, \hat{B}] = -\hat{C} \qquad [\hat{B}, \hat{C}] = \hat{A} \qquad [\hat{C}, \hat{A}] = \hat{B}. \tag{1.9}$$

Equation (1.9) represents a closed Lie algebra basis and this of course gives us an advantage when dealing with such a problem, which may be regarded as the most generalized Hamiltonian for three modes interaction [26]. It is interesting to refer to [26], where the transformed Hamiltonian (1.7) has been considered and the wavefunction is obtained by using the Lie algebra technique. Now let us connect this model with the system of a directional coupler with parametric amplification [27, 28]. To see that we shall write the equations describing the non-classical evolution of the fields in the presence of a strong and non-depleted pump as follows

$$\frac{\mathrm{d}a}{\mathrm{d}z} = -\mathrm{i}kb - \mathrm{i}gc^\dagger \tag{1.10a}$$

$$\frac{\mathrm{d}c^\dagger}{\mathrm{d}z} = \mathrm{i}ga \tag{1.10b}$$

$$\frac{\mathrm{d}b}{\mathrm{d}z} = -\mathrm{i}ka - \mathrm{i}ge^\dagger \tag{1.10c}$$

$$\frac{\mathrm{d}e^\dagger}{\mathrm{d}z} = \mathrm{i}gb \tag{1.10d}$$

where a and b are the annihilation operators for the fields of the same frequency, $c^\dagger$ and $e^\dagger$ are the creation operators of the modes coupled through the amplifying mechanism to modes a and b respectively, while z is a dimension of space which in general depends on the time. From the above equations we can write the effective momentum operator which describes such a system as

$$\frac{H}{\hbar} = g(a^\dagger c^\dagger + ac) + g(be + b^\dagger e^\dagger) + k(ab^\dagger + ba^\dagger) \tag{1.11}$$

where k and g are the coupling constant and an amplification factor respectively. By taking the operators c and e to equal each other such that the operator c has the same properties of the operator e, and considering that all the coupling parameters are different, we then find that equation (1.11) will reduce to equation (1.7) provided we take the phases ϕ_i in equation (1.5) to be $3\pi/2$ [26].

In section 2, we shall derive the solution of the equations of motion in the Heisenberg picture. In section 3 we shall discuss the bunching and antibunching through the Glauber second-order correlation function. Section 4 will be devoted to discussing the squeezing phenomena, while in section 5 we shall consider the quasiprobability distribution function. Finally, we give our conclusions in section 6.

2. The equations of motion and their solutions

In order to study the dynamics of the system we have to find the solution of the equations of motion in the Heisenberg picture. In this section we shall aim at finding this solution for the Hamiltonian given by equation (1.5). The Heisenberg equations of motion for any operator $\hat{O}$ is given by

$$\frac{\mathrm{d}\hat{O}}{\mathrm{d}t} = \frac{1}{\mathrm{i}\hbar}[\hat{O}, H] + \frac{\partial\hat{O}}{\partial t}. \tag{2.1}$$

Therefore the equations of motion for the Hamiltonian (1.7) can thus be written

$$\frac{\mathrm{d}A_1}{\mathrm{d}t} = \lambda_1 A_2^\dagger + \lambda_2 A_3^\dagger \tag{2.2a}$$

$$\frac{\mathrm{d}A_2}{\mathrm{d}t} = \lambda_1 A_1^\dagger + \lambda_3 A_3 \tag{2.2b}$$

$$\frac{\mathrm{d}A_3}{\mathrm{d}t} = \lambda_2 A_1^\dagger - \lambda_3 A_2. \tag{2.2c}$$

By invoking the Laplace transformation of these equations, we obtain the solution of the corresponding set of algebraic equations; performing the inverse transformation we have the solution of the form

$$A_1(t) = f_1(t)A_1(0) + f_2(t)A_2^\dagger(0) + f_3(t)A_3^\dagger(0) \tag{2.3a}$$

$$A_2(t) = h_1(t)A_2(0) + h_2(t)A_3(0) + h_3(t)A_1^\dagger(0) \tag{2.3b}$$

$$A_3(t) = k_1(t)A_3(0) + k_2(t)A_2(0) + k_3(t)A_1^\dagger(0) \tag{2.3c}$$

where

$$f_1(t) = \cos gt + 2\frac{\lambda_3^2}{g^2}\sin^2\frac{gt}{2} \tag{2.4a}$$

$$f_2(t) = \frac{\lambda_1}{g}\sin gt - 2\frac{\lambda_2\lambda_3}{g^2}\sin^2\frac{gt}{2} \tag{2.4b}$$

$$f_3(t) = \frac{\lambda_2}{g}\sin gt + 2\frac{\lambda_1\lambda_3}{g^2}\sin^2\frac{gt}{2} \tag{2.4c}$$

while

$$h_1(t) = \cos gt - \frac{2\lambda_2^2}{g^2}\sin^2\frac{gt}{2} \tag{2.5a}$$

$$h_2(t) = \frac{\lambda_3}{g}\sin gt + 2\frac{\lambda_1\lambda_2}{g^2}\sin^2\frac{gt}{2} \tag{2.5b}$$

$$h_3(t) = \frac{\lambda_1}{g}\sin gt + 2\frac{\lambda_2\lambda_3}{g^2}\sin^2\frac{gt}{2} \tag{2.5c}$$

and

$$k_1(t) = \cos gt - \frac{2\lambda_1^2}{g^2}\sin^2\frac{gt}{2} \tag{2.6a}$$

$$k_2(t) = -\frac{\lambda_3}{g}\sin gt + 2\frac{\lambda_1\lambda_2}{g^2}\sin^2\frac{gt}{2} \tag{2.6b}$$

$$k_3(t) = -\frac{\lambda_2}{g}\sin gt - 2\frac{\lambda_1\lambda_3}{g^2}\sin^2\frac{gt}{2} \tag{2.6c}$$

and $g = \sqrt{\lambda_3^2 - \lambda_1^2 - \lambda_2^2}$.

Equations (2.4)–(2.6) satisfy the following identities

$$f_1^2(t) - f_2^2(t) - f_3^2(t) = 1 \tag{2.7a}$$

$$h_1^2(t) + h_2^2(t) - h_3^2(t) = 1 \tag{2.7b}$$

$$k_1^2(t) + k_2^2(t) - k_3^2(t) = 1 \tag{2.7c}$$

and

$$f_1(t)h_3(t) = f_2(t)h_1(t) + h_2(t)f_3(t) \tag{2.8a}$$

$$f_1(t)k_3(t) = f_2(t)k_2(t) + f_3(t)k_1(t) \tag{2.8b}$$

$$h_3(t)k_3(t) = h_1(t)k_2(t) + h_2(t)k_1(t). \tag{2.8c}$$

These equations will be used in the forthcoming calculations.

Now, by using equations (1.6) and (2.3) we can write the general solution of the equations of motion in Heisenberg picture as follows

$$a_1(t) = \mathrm{e}^{-\mathrm{i}\omega_1 t}[f_1(t)a_1(0) + f_2(t)a_2^\dagger(0) + f_3(t)a_3^\dagger(0)] \tag{2.9a}$$

$$a_2(t) = \mathrm{e}^{-\mathrm{i}\omega_2 t}[h_1(t)a_2(0) + h_2(t)a_3(0) + h_3(t)a_1^\dagger(0)] \tag{2.9b}$$

$$a_3(t) = \mathrm{e}^{-\mathrm{i}\omega_3 t}[k_1(t)a_3(0) + k_2(t)a_2(0) + k_3(t)a_1^\dagger(0)]. \tag{2.9c}$$

We should point out that the above result has been obtained under the condition $\lambda_3^2 > \lambda_1^2+\lambda_2^2$, however, an alternative result may be obtained for the case $\lambda_3^2 < \lambda_1^2 + \lambda_2^2$, if one uses the analytic continuation $g \to \mathrm{i}\lambda$, with $\lambda = \sqrt{\lambda_1^2 + \lambda_2^2 - \lambda_3^2}$. In the following section we shall use the result obtained in this section to discuss some statistical properties of the photon numbers related to the Hamiltonian (1.5).

3. Field fluctuations and correlation functions

In this section we shall employ the Glauber second-order correlation function to discuss some statistical properties of the photon numbers related to the Hamiltonian model (1.5). This will be done in two different ways; the first is to use the number state as the initial state, while the second is to use the coherent state as the initial state. To do so we shall calculate the expectation value of the photon numbers $\langle n_i(t)\rangle$ as well as the second moment of the photon numbers $\langle n_i^2(t)\rangle$, $i = 1, 2, 3$. The calculations of these quantities with respect to the number state $|n_i\rangle$ as the initial state gives

$$\langle n_1(t)\rangle = f_1^2(t)\bar{n}_1 + f_2^2(t)(\bar{n}_2 + 1) + f_3^2(t)(\bar{n}_3 + 1) \tag{3.1a}$$

$$\langle n_2(t)\rangle = h_1^2(t)\bar{n}_2 + h_2^2(t)\bar{n}_3 + h_3^2(t)(\bar{n}_1 + 1) \tag{3.1b}$$

$$\langle n_3(t)\rangle = k_1^2(t)\bar{n}_3 + k_2^2(t)\bar{n}_2 + k_3^2(t)(\bar{n}_1 + 1) \tag{3.1c}$$

and

$$\begin{aligned}\langle n_1^2(t)\rangle = {} & f_1^4(t)\bar{n}_1^2 + f_2^4(t)(\bar{n}_2 + 1)^2 + f_3^4(t)(\bar{n}_3 + 1)^2 + f_1^2(t)f_2^2(t)(4\bar{n}_1\bar{n}_2 + 3\bar{n}_1 + \bar{n}_2 + 1) \\ & + f_2^2(t)f_3^2(t)(4\bar{n}_2\bar{n}_3 + 3\bar{n}_2 + 3\bar{n}_3 + 2) + f_1^2(t)f_3^2(t)(4\bar{n}_1\bar{n}_3 + 3\bar{n}_1 + \bar{n}_3 + 1)\end{aligned} \tag{3.2a}$$

$$\langle n_2^2(t)\rangle = h_1^4(t)\bar{n}_2^2 + h_2^4(t)\bar{n}_3^2 + h_3^4(t)(\bar{n}_1+1)^2 + h_1^2(t)h_2^2(t)(4\bar{n}_2\bar{n}_3+\bar{n}_2+\bar{n}_3) + h_2^2(t)h_3^2(t)(4\bar{n}_1\bar{n}_3+3\bar{n}_3+\bar{n}_1+1) + h_1^2(t)h_3^2(t)(4\bar{n}_1\bar{n}_2+3\bar{n}_2+\bar{n}_1+1) \tag{3.2b}$$

and

$$\langle n_3^2(t)\rangle = k_1^4\bar{n}_3^2 + k_1^4(t)\bar{n}_2^2 + k_3^4(t)(\bar{n}_1+1)^2 + k_1^2(t)k_2^2(t)(4\bar{n}_2\bar{n}_3+\bar{n}_2+\bar{n}_3) + k_2^2(t)k_3^2(t)(4\bar{n}_1\bar{n}_2+3\bar{n}_2+\bar{n}_1+1) + k_1^2(t)k_3^2(t)(4\bar{n}_1\bar{n}_3+3\bar{n}_3+\bar{n}_1+1) \tag{3.2c}$$

where $\bar{n}_i$, $i = 1, 2, 3$ are the mean photon numbers with respect to the state $|n_i\rangle$ at $t = 0$. From equations (3.1) and (3.2) we can calculate the photon number variances to take the following expressions

$$\overline{\Delta n_1}^2 = f_1^2(t)f_2^2(t)(2\bar{n}_1\bar{n}_2+\bar{n}_1+\bar{n}_2+1) + f_3^2(t)f_2^2(t)(2\bar{n}_2\bar{n}_3+\bar{n}_2+\bar{n}_3) + f_1^2(t)f_3^2(t)(2\bar{n}_1\bar{n}_3+\bar{n}_1+\bar{n}_3+1) \tag{3.3a}$$

$$\overline{\Delta n_2}^2 = h_1^2(t)h_2^2(t)(2\bar{n}_2\bar{n}_3+\bar{n}_2+\bar{n}_3) + h_2^2(t)h_3^2(t)(2\bar{n}_1\bar{n}_3+\bar{n}_3+\bar{n}_1+1) + h_1^2(t)h_3^2(t)(2\bar{n}_1\bar{n}_2+\bar{n}_2+\bar{n}_1+1) \tag{3.3b}$$

and

$$\overline{\Delta n_3}^2 = k_1^2(t)k_2^2(t)(2\bar{n}_2\bar{n}_3+\bar{n}_2+\bar{n}_3) + k_1^2(t)k_3^2(t)(2\bar{n}_1\bar{n}_3+\bar{n}_1+\bar{n}_3+1) + k_2^2(t)k_3^2(t)(2\bar{n}_1\bar{n}_2+\bar{n}_1+\bar{n}_2+1). \tag{3.3c}$$

We shall now use the result given by the above equations to discuss the bunching and antibunching. This can be done by examining the Glauber second-order correlation function for the three modes which is defined by [8]

$$g_i^{(2)}(t) = 1 + \frac{[\overline{\Delta n_i}^2(t) - \langle n_i(t)\rangle]}{\langle n_i(t)\rangle^2} \qquad i = 1, 2, 3. \tag{3.4}$$

Now let us examine the quantity $\overline{\Delta n_i}^2 - \langle n_i\rangle$ against the vacuum state, in this case we have

$$\overline{\Delta n_1}^2 - \langle n_1\rangle = (f_1^2(t) - 1)^2 > 0 \tag{3.5a}$$

$$\overline{\Delta n_2}^2 - \langle n_2\rangle = h_3^4(t) > 0 \tag{3.5b}$$

$$\overline{\Delta n_3}^2 - \langle n_3\rangle = k_3^4(t) > 0. \tag{3.5c}$$

The above equations show a bunching behaviour of the system for all time $t > 0$. On the other hand, if we examine the Glauber second-order correlation functions (3.4) against the number state $\prod_{i=1}^{3}|n_i\rangle$, we can easily see the bunching, antibunching as well as coherence behaviour. In fact this behaviour would appear as a result of the existence of the oscillating function in both the photon number and photon number variances, see figures 1(a)–(c), where we have plotted the function $g_1^{(2)}(t)$ against time. It is worthwhile referring to the photon number $\bar{n}_i$ and the coupling parameters λ_i which are controlling the behaviour of the correlation functions. For example, if we fix the value of the parameters λ_i such that $\lambda_3^2 > \lambda_1^2 + \lambda_2^2$, and by changing the value of the photon number $\bar{n}_i$ such that $\bar{n}_1 = \bar{n}_3$, and taking $\bar{n}_2$ to be large compared with both $\bar{n}_1$ and $\bar{n}_3$, then the function $g_1^{(2)}(t)$ shows partially coherence behaviour, with a maximum value at 1.65, see figure 1(a). However, when we increase the value of $\bar{n}_3$ and decrease the value of $\bar{n}_2$, we find that $g_1^{(2)}(t)$ does not reach the previous value, but it reaches the value 1.4 faster than in the previous case, see figure 1(b). The same behaviour will be seen when we take the value of $\bar{n}_1$ to be

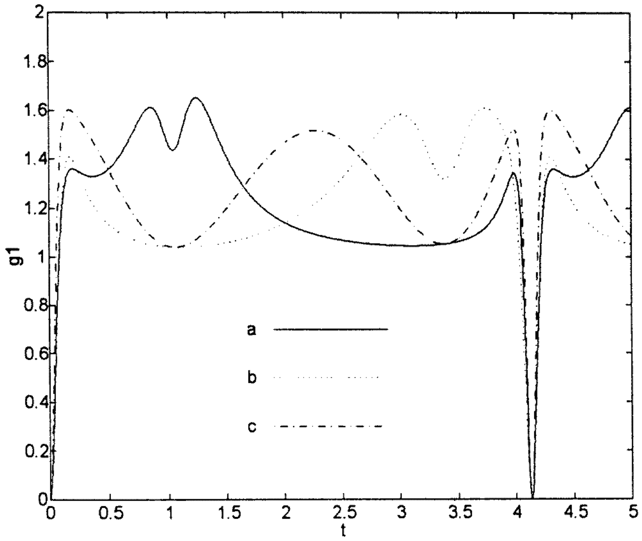

Figure 1. The second-order correlation function $g_1^{(2)}$ with respect to the number state against time, with (a) $n_i = (1, 100, 1)$, $\lambda_i = (0.9, 0.7, 1.9)$, $i = 1, 2, 3$, (b) as (a) but with $n_i = (1, 10, 100)$, (c) as (a) but with $n_i = (1, 100, 100)$.

small, compared with the large value of $\bar{n}_2$ and $\bar{n}_3$, see figure 1(c), however, we can notice that the value of $g_1^{(2)}(t)$ will increase faster than the other two cases in a short period of time, but it still has partially coherence behaviour with a maximum value less than the first case. Here we may point out that for some period of time the correlation function $g_1^{(2)}(t)$ also shows antibunching behaviour as can be seen in figures 1(a)–(c). These periods are actually smaller than the period of bunching. The above discussion can also be applied to $g_2^{(2)}(t)$ and $g_3^{(2)}(t)$, but with different periods of oscillations. On the other hand, if we take $\lambda_1^2 + \lambda_2^2 > \lambda_3^2$ the correlation function $g_1^{(2)}(t)$ exhibits antibunching behaviour for a short period of time when we take small values for both $\bar{n}_1$ and $\bar{n}_2$ and a large value of $\bar{n}_3$ (see figure 2(a)). However, the situation is different when we increase the value of the photon number $\bar{n}_1$ and decrease the value of $\bar{n}_2$ and $\bar{n}_3$ where the function $g_1^{(2)}(t)$ shows coherence behaviour (see figure 2(b)). Finally if we take the value of all n_i to be large, then the system will show bunched behaviour (see figure 2(c)). To complete this section we turn our attention to examining the correlation function $g_i^{(2)}(t)$, $i = 1, 2, 3$, taking into consideration the coherent state as an initial state. In this case we find that the photon number $\langle n_i \rangle$ takes the form

$$\begin{aligned}\langle n_1(t)\rangle =\ & f_1^2(t)|\alpha_1|^2 + f_2^2(t)(|\alpha_2|^2+1) + f_3^2(t)(|\alpha_3|^2+1) + f_1(t)f_2(t)(\alpha_1\alpha_2+\alpha_1^*\alpha_2^*)\\ & + f_2(t)f_3(t)(\alpha_2\alpha_3^*+\alpha_2^*\alpha_3) + f_1(t)f_3(t)(\alpha_1^*\alpha_3^*+\alpha_1\alpha_3) \qquad (3.6a)\end{aligned}$$

$$\begin{aligned}\langle n_2(t)\rangle =\ & h_1^2(t)|\alpha_2|^2 + h_2^2(t)|\alpha_3|^2 + h_3^2(t)(|\alpha_1|^2+1) + h_1(t)h_2(t)(\alpha_2^*\alpha_3+\alpha_2\alpha_3^*)\\ & + h_2(t)h_3(t)(\alpha_1^*\alpha_3^*+\alpha_1\alpha_3) + h_1(t)h_3(t)(\alpha_1^*\alpha_2^*+\alpha_1\alpha_2) \qquad (3.6b)\end{aligned}$$

$$\begin{aligned}\langle n_3(t)\rangle =\ & k_1^2(t)|\alpha_3|^2 + k_2^2(t)|\alpha_2|^2 + k_3^2(|\alpha_1|^2+1) + k_1(t)k_2(t)(\alpha_2\alpha_3^*+\alpha_2^*\alpha_3)\\ & + k_2(t)k_3(t)(\alpha_1^*\alpha_2^*+\alpha_1\alpha_2) + k_1(t)k_3(t)(\alpha_1^*\alpha_3^*+\alpha_1\alpha_3) \qquad (3.6c)\end{aligned}$$

and the calculations of the second moment $\langle n_i^2 \rangle$ lead to the following expressions

$$\langle n_1^2(t)\rangle = f_1^4(t)(|\alpha_1|^4+|\alpha_1|^2) + f_2^4(t)(|\alpha_2|^4+3|\alpha_2|^2+1) + f_3^4(t)(|\alpha_3|^4+3|\alpha_3|^2+1)$$

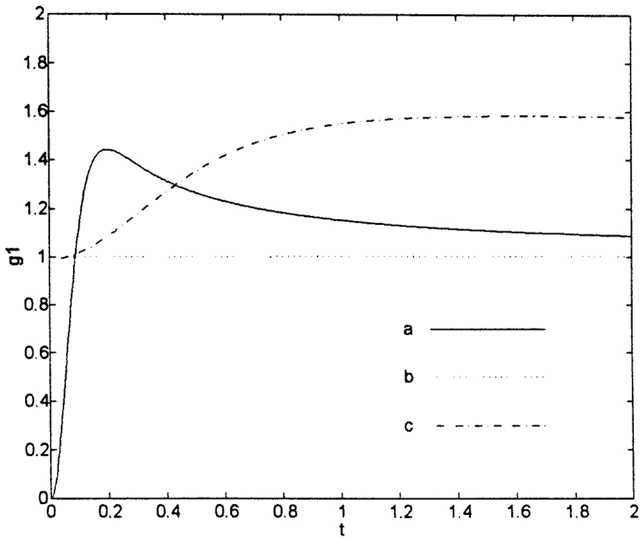

Figure 2. The correlation function $g_1^{(2)}$ against time with $\lambda_i = (0.9, 0.7, 0.9)$. (*a*) $n_i = (1, 10, 100)$, (*b*) $n_i = (1000, 1, 1)$, (*c*) $n_i = (100, 100, 100)$.

$$
\begin{aligned}
&+f_1^2(t)f_2^2(t)[4|\alpha_1|^2|\alpha_2|^2 + 3|\alpha_1|^2 + |\alpha_2|^2 + \alpha_1^2\alpha_2^2 + \alpha_1^{*2}\alpha_2^{*2} + 1]\\
&+f_1^2(t)f_3^2(t)[4|\alpha_1|^2|\alpha_3|^2 + 3|\alpha_1|^2 + |\alpha_3|^2 + \alpha_1^2\alpha_3^2 + \alpha_1^{*2}\alpha_3^{*2} + 1]\\
&+f_2^2(t)f_3^2(t)[4|\alpha_2|^2|\alpha_3|^2 + 3|\alpha_2|^2 + 3|\alpha_3|^2 + \alpha_2^{*2}\alpha_3^2 + \alpha_3^{*2}\alpha_2^2 + 1]\\
&+f_1^3(t)(2|\alpha_1|^2 + 1)[f_2(t)(\alpha_1\alpha_2 + \alpha_1^*\alpha_2^*) + f_3(t)(\alpha_1\alpha_3 + \alpha_1^*\alpha_3^*)]\\
&+f_2^3(t)(2|\alpha_2|^2 + 3)[f_1(t)(\alpha_1\alpha_2 + \alpha_1^*\alpha_2^*) + f_3(t)(\alpha_2^*\alpha_3 + \alpha_3^*\alpha_2)]\\
&+f_3^3(t)(2|\alpha_3|^2 + 3)[f_1(t)(\alpha_1\alpha_3 + \alpha_1^*\alpha_3^*) + f_2(t)(\alpha_2\alpha_3^* + \alpha_2^*\alpha_3)]\\
&+f_1^2(t)f_2(t)f_3(t)[(4|\alpha_1|^2 + 1)(\alpha_2^*\alpha_3 + \alpha_3^*\alpha_2) + 2(\alpha_1^2\alpha_2\alpha_3 + \alpha_1^{*2}\alpha_2^*\alpha_3^*)]\\
&+f_1(t)f_2^2(t)f_3(t)[(4|\alpha_2|^2 + 3)(\alpha_1\alpha_3 + \alpha_1^*\alpha_3^*) + 2(\alpha_1^2\alpha_2^2\alpha_3^* + \alpha_1^*\alpha_2^{*2}\alpha_3)]\\
&+f_1(t)f_2(t)f_3^2(t)[(4|\alpha_3|^2 + 3)(\alpha_1\alpha_2 + \alpha_1^*\alpha_2^*) + 2(\alpha_1^*\alpha_3^{*2}\alpha_2 + \alpha_1\alpha_3^2\alpha_2^*)]
\end{aligned}
\tag{3.7a}
$$

$$
\begin{aligned}
\langle n_2^2(t)\rangle = {}& h_1^4(t)(|\alpha_2|^4 + |\alpha_2|^2) + h_2^4(t)(|\alpha_3|^4 + |\alpha_3|^2) + h_3^4(t)(|\alpha_1|^4 + 3|\alpha_1|^2 + 1)\\
&+h_1^2(t)h_2^2(t)[4|\alpha_2|^2|\alpha_3|^2 + |\alpha_3|^2 + |\alpha_2|^2 + \alpha_2^{*2}\alpha_3^2 + \alpha_3^{*2}\alpha_2^2]\\
&+h_1^2(t)h_3^2(t)[4|\alpha_1|^2|\alpha_2|^2 + |\alpha_1|^2 + 3|\alpha_2|^2 + 1 + \alpha_1^{*2}\alpha_2^{*2} + \alpha_1^2\alpha_2^2]\\
&+h_2^2(t)h_3^2(t)[4|\alpha_1|^2|\alpha_3|^2 + |\alpha_1|^2 + 3|\alpha_3|^2 + 1 + \alpha_1^{*2}\alpha_3^{*2} + \alpha_1^2\alpha_3^2]\\
&+h_1^3(t)(2|\alpha_2|^2 + 1)[h_2(t)(\alpha_2\alpha_3^* + \alpha_2^*\alpha_3) + h_3(t)(\alpha_1\alpha_2 + \alpha_1^*\alpha_2^*)]\\
&+h_2^3(t)(2|\alpha_3|^2 + 1)[h_1(t)(\alpha_2^*\alpha_3 + \alpha_3^*\alpha_2) + h_3(t)(\alpha_1\alpha_3 + \alpha_1^*\alpha_3^*)]\\
&+h_3^3(t)(2|\alpha_1|^2 + 3)[h_1(t)(\alpha_1^*\alpha_2^* + \alpha_1\alpha_2) + h_2(t)(\alpha_1\alpha_3 + \alpha_1^*\alpha_3^*)]\\
&+h_1^2(t)h_2(t)h_3(t)[(4|\alpha_2|^2 + 1)(\alpha_1\alpha_3 + \alpha_1^*\alpha_3^*) + 2(\alpha_1^*\alpha_2^{*2}\alpha_3 + \alpha_1\alpha_2^2\alpha_3^*)]\\
&+h_1(t)h_2^2(t)h_3(t)[(4|\alpha_3|^2 + 1)(\alpha_1^*\alpha_2^* + \alpha_1\alpha_2) + 2(\alpha_1\alpha_2^*\alpha_3^2 + \alpha_1^*\alpha_2\alpha_3^{*2})]\\
&+h_1(t)h_2(t)h_3^2(t)[(4|\alpha_1|^2 + 3)(\alpha_2^*\alpha_3 + \alpha_2\alpha_3^*) + 2(\alpha_1^2\alpha_2\alpha_3 + \alpha_1^{*2}\alpha_2^*\alpha_3^*)]
\end{aligned}
\tag{3.7b}
$$

$$
\langle n_3^2(t)\rangle = k_1^4(t)(|\alpha_3|^4 + |\alpha_3|^2) + k_2^4(t)(|\alpha_2|^4 + |\alpha_2|^2) + k_3^4(t)(|\alpha_1|^4 + 3|\alpha_1|^2 + 1)
$$

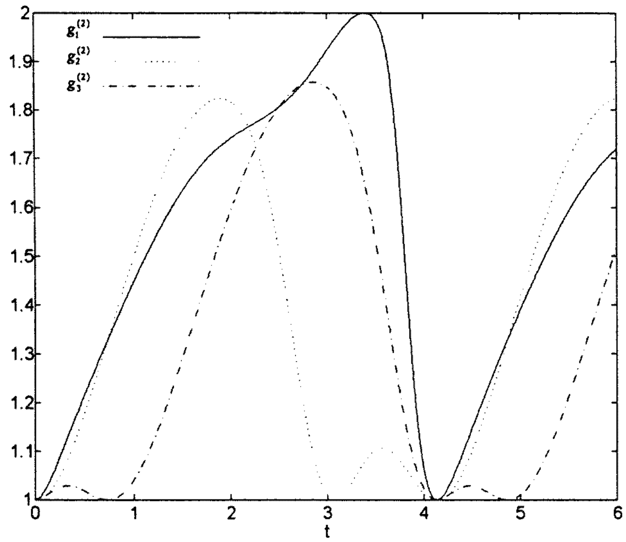

Figure 3. The correlation function $g_i^{(2)}$ with respect to the coherent state against time, with $n_i = (1, 2, 1)$, $\lambda_i = (0.9, 0.7, 1.9)$ and $\delta_i = (\pi, \pi, \pi/2)$.

$$\begin{aligned}
&+k_1^2(t)k_2^2(t)(4|\alpha_2|^2|\alpha_3|^2 + \alpha_2^{*2}\alpha_3^2 + \alpha_3^{*2}\alpha_2^2 + |\alpha_2|^2 + |\alpha_3|^2)\\
&+k_1^2(t)k_3^2(t)(4|\alpha_1|^2|\alpha_3|^2 + \alpha_1^{*2}\alpha_3^{*2} + \alpha_1^2\alpha_3^2 + |\alpha_1|^2 + 3|\alpha_3|^2 + 1)\\
&+k_2^2(t)k_3^2(t)(4|\alpha_1|^2|\alpha_2|^2 + \alpha_1^{*2}\alpha_2^{*2} + \alpha_1^2\alpha_2^2 + |\alpha_1|^2 + 3|\alpha_2|^2 + 1)\\
&+k_1^3(t)(2|\alpha_3|^2 + 1)[k_2(t)(\alpha_2\alpha_3^* + \alpha_2^*\alpha_3) + k_3(t)(\alpha_1^*\alpha_3^* + \alpha_1\alpha_3)]\\
&+k_2^3(t)(2|\alpha_2|^2 + 1)[k_1(t)(\alpha_2^*\alpha_3 + \alpha_2\alpha_3^*) + k_3(t)(\alpha_1\alpha_2 + \alpha_1^*\alpha_2^*)]\\
&+k_3^3(t)(2|\alpha_1|^2 + 3)[k_1(t)(\alpha_1^*\alpha_3^* + \alpha_1\alpha_3) + k_2(t)(\alpha_1\alpha_2 + \alpha_1^*\alpha_2^*)]\\
&+k_1^2(t)k_2(t)k_3(t)[(4|\alpha_3|^2 + 1)(\alpha_1\alpha_2 + \alpha_1^*\alpha_2^*) + 2(\alpha_1^*\alpha_2\alpha_3^{*2} + \alpha_1\alpha_2^*\alpha_3^2)]\\
&+k_1(t)k_2^2(t)k_3(t)[(4|\alpha_2|^2 + 1)(\alpha_1^*\alpha_3^* + \alpha_1\alpha_3) + 2(\alpha_1\alpha_2^2\alpha_3^* + \alpha_1^*\alpha_2^{*2}\alpha_3)]\\
&+k_1(t)k_2(t)k_3^2(t)[(4|\alpha_1|^2 + 3)(\alpha_3^*\alpha_2 + \alpha_2^*\alpha_3) + 2(\alpha_1^{*2}\alpha_2^*\alpha_3^* + \alpha_1^2\alpha_2\alpha_3)].
\end{aligned} \tag{3.7c}$$

In figures 3–7 we have plotted the functions $g_j^{(2)}(t)$ against time t, for $\lambda_3^2 > \lambda_1^2 + \lambda_2^2$. For different values of $|\alpha_j|$ and δ_j where $\alpha_j = |\alpha_j|e^{-i\delta j}$, as one should expect, the value of the functions $g_j^{(2)}(t)$, $j = 1, 2, 3$, will be affected by the values of $|\alpha_j|$ and δ_j. For example, we find that for small values of $|\alpha_j|$, such that $(1, \sqrt{2}, 1)$ and for fixing values of $\delta_j(\pi, \pi, \pi/2)$, the function $g_1^{(2)}(t)$ reaches the value 2, while the other two functions show partially coherence behaviour, see figure 3. In contrast, when we take the values of $|\alpha_j|$ to be $(\sqrt{2}, 1, 1)$ with the same values of δ_j, we find that the function $g_1^{(2)}(t)$ exhibits partially coherence behaviour while the other two functions show thermal distribution (see figure 4). However, as we increase the value of the photon numbers, the correlation function $g_1^{(2)}(t)$ decreases its value and does not reach the value of thermal distribution for some values of the phases δ_j. This can be seen if we take $|\alpha_j|$ such that $(10, 1, 1)$ and the phases δ_j with the values $(\pi/2, \pi/2, \pi)$, the function $g_1^{(2)}(t)$ becomes approximately one, while $g_2^{(2)}(t)$ and $g_3^{(2)}(t)$ getting sharpers and the period of reaching large values is small, see figure 5. On the other hand, if we set $|\alpha_j|$ such that $(1, 10, 1)$, with the same value of δ_j as in the previous case,

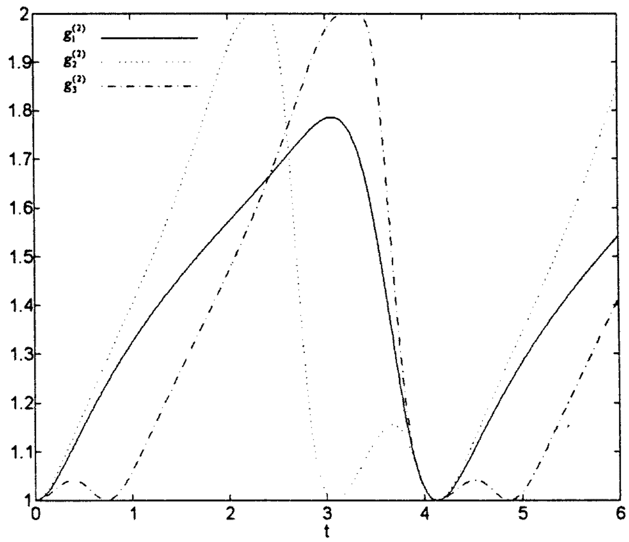

Figure 4. As in figure 3 but with $n_i = (2, 1, 1)$, and $\delta_i = (\pi, \pi, \pi/2)$.

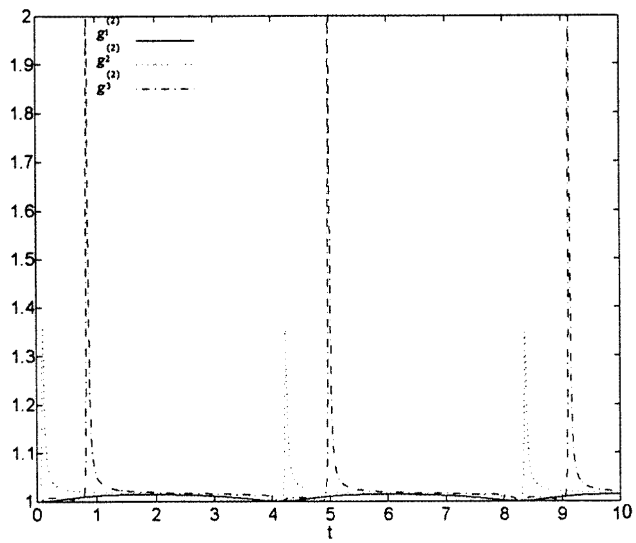

Figure 5. As in figure 3 but with $n_i = (100, 1, 1)$, and $\delta_i = (\pi/2, \pi/2, \pi)$.

then the value of the function $g_1^{(2)}(t)$ increases as well as the other two functions, but none of them reach thermal distribution, see figure 6. When we examined the case $\lambda_3^2 < \lambda_1^2 + \lambda_2^2$, we found for small values of the photon numbers $n_i = 1$ and $\delta_i = (\pi, 0, 0)$, the functions $g_i^{(2)}$ show thermal distribution behaviour. This situation is different when we take the value of the photon numbers n_2 to be large compared with n_1 and n_2 with different values of the phases δ_i, where we have observed partially coherence behaviour, see figures 7(a) and (b). Finally we would like to point out that comparing the function $g_j^{(2)}(t)$ in the number state with the coherent state, we can conclude that the function in the number state shows antibunching for some period of time while the function in the coherent state does not exhibit this phenomena.

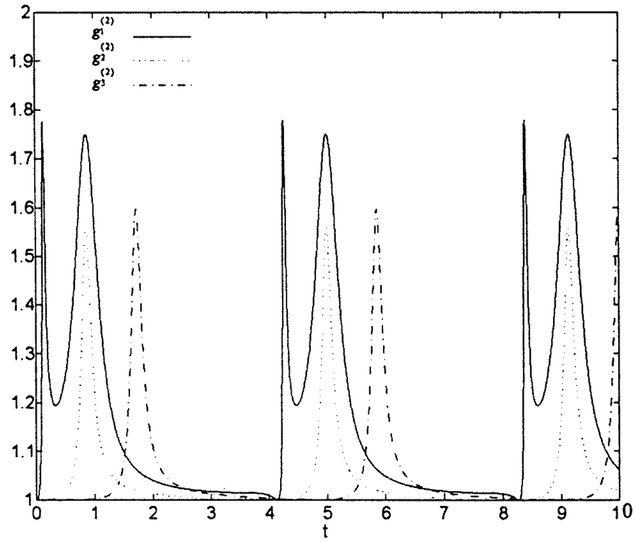

Figure 6. As in figure 5 but with $n_i = (1, 100, 1)$.

4. Squeezing

In this section we turn our attention to considering the squeezing phenomena. This phenomena represents one of the most interesting phenomena in the field of quantum optics [29]. If we now define two quadrature operators for the field, such that $X = (a_1 + a_1^\dagger)/\sqrt{2}$, and $Y = (a_1 - a_1^\dagger)/\mathrm{i}\sqrt{2}$, then the system under consideration does not exhibit squeezing, however, if we define the quadrature operators for the field to be the combination between two or more modes, then the phenomena of squeezing can easily be observed. To see that, let us define two quadrature operators, such that

$$X_1 = \tfrac{1}{2}[(a_1 + a_2) + (a_1^\dagger + a_2^\dagger)] \tag{4.1a}$$

$$Y_1 = \frac{1}{2\mathrm{i}}[(a_1 + a_2) - (a_1^\dagger + a_2^\dagger)] \tag{4.1b}$$

these two quadrature operators satisfy the commutation relation

$$[X_1, Y_1] = i. \tag{4.2}$$

From equations (4.1a), (4.1b) and (2.7a), (2.7b) we have

$$\overline{\Delta X_1^2} = \tfrac{1}{2}[f_1^2(t) + h_3^2(t) + 2f_1(t)h_3(t)\cos(\omega_1 + \omega_2)t] \tag{4.3a}$$

$$\overline{\Delta Y_1^2} = \tfrac{1}{2}[f_1^2(t) + h_3^2(t) - 2f_1(t)h_3(t)\cos(\omega_1 + \omega_2)t] \tag{4.3b}$$

and the uncertainty product leads to

$$\overline{\Delta X_1} \cdot \overline{\Delta Y_1} = \tfrac{1}{2}[(f_1^2(t) - h_3^2(t))^2 + 4f_1^2(t)h_3^2(t)\sin^2(\omega_1 + \omega_2)t]^{\frac{1}{2}} \tag{4.3c}$$

where $f_1(t)$ and $h_3(t)$ are functions of time given by equations (2.4a) and (2.5c) respectively. Equations (4.1) may be extended to include three modes instead of two modes. In this case we can define the following quadrature operators

$$X_2 = \frac{1}{\sqrt{6}}[(a_1 + a_2 + a_3) + (a_1^\dagger + a_2^\dagger + a_3^\dagger)] \tag{4.4a}$$

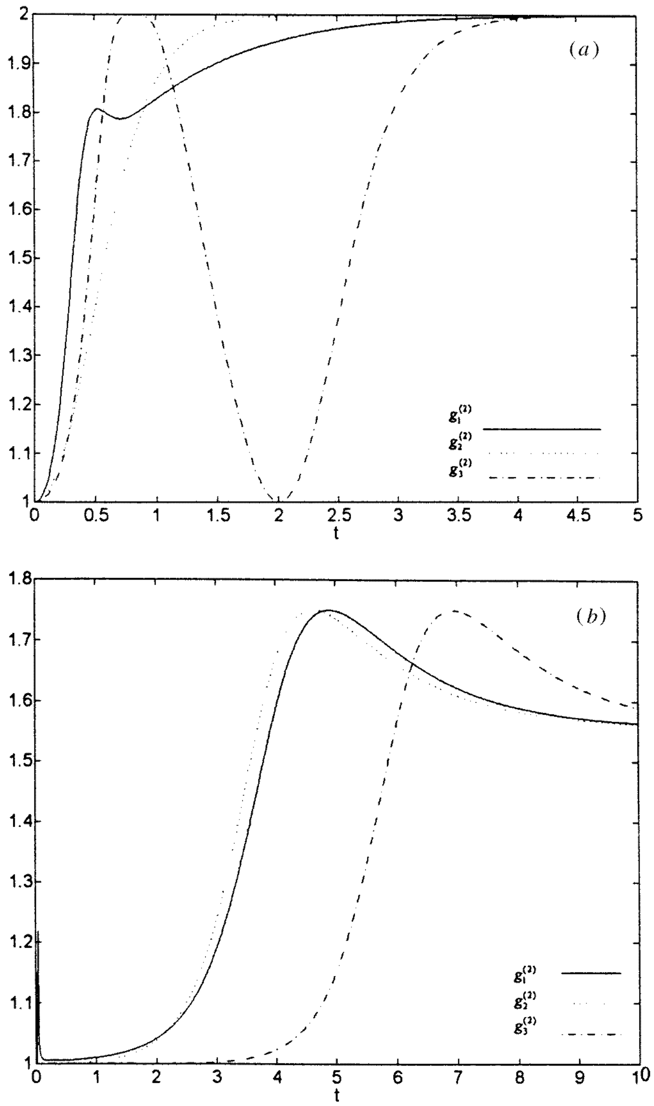

Figure 7. (*a*) As in figure 3 but with $n_i = (1, 1, 1)$, and $\lambda_i = (0.9, 0.7, 0.9)$ and $\delta_i = (\pi, 0, 0)$. (*b*) As in (*a*) but with $n_i = (1, 1000, 1)$, and $\delta_i = (\pi/2, \pi/2, \pi)$.

$$Y_2 = \frac{1}{\mathrm{i}\sqrt{6}}[(a_1 + a_2 + a_3) - (a_1^{\dagger} + a_2^{\dagger} + a_3^{\dagger})] \tag{4.4b}$$

which satisfy the commutation relation given by equation (4.2). The calculation for quadrature variances gives

$$\begin{aligned}\overline{\Delta X}_2^2 = \tfrac{1}{6}[1 &+ 2(f_1^2(t) + h_3^2(t) + k_3^2(t)) + 4f_1(t)k_3(t)\cos(\omega_1+\omega_3)t \\ &+ 4f_1(t)h_3(t)\cos(\omega_1+\omega_2)t + 4h_3(t)k_3(t)\cos(\omega_2-\omega_3)t]\end{aligned} \tag{4.5a}$$

$$\begin{aligned}\overline{\Delta Y}_2^2 = \tfrac{1}{6}[1 &+ 2(f_1^2(t) + h_3^2(t) + k_3^2(t)) - 4f_1(t)k_3(t)\cos(\omega_1+\omega_3)t \\ &- 4f_1(t)h_3(t)\cos(\omega_1+\omega_2)t + 4h_3(t)k_3(t)\cos(\omega_2-\omega_3)t].\end{aligned} \tag{4.5b}$$

Alternatively we can define the quadrature operators X_3 and Y_3 to satisfy the commutation relations as in equation (4.2) such that

$$\sqrt{6}X_3 = [(a_1 - a_2 - a_3) + (a_1^\dagger - a_2^\dagger - a_3^\dagger)] \tag{4.6a}$$

$$\mathrm{i}\sqrt{6}Y_3 = [(a_1 - a_2 - a_3) - (a_1^\dagger - a_2^\dagger - a_3^\dagger)]. \tag{4.6b}$$

Hence, the quadrature variances in this case take the form

$$\begin{aligned}\overline{\Delta X_3^2} = \tfrac{1}{6}[1 &+ 2(f_1^2(t) + h_3^2(t) + k_3^2(t)) + 4f_1(t)k_3(t)\cos(\omega_1+\omega_3)t \\ &-4f_1(t)h_3(t)\cos(\omega_1+\omega_2)t - 4h_3(t)k_3(t)\cos(\omega_2-\omega_3)t]\end{aligned} \tag{4.7a}$$

$$\begin{aligned}\overline{\Delta Y_3^2} = \tfrac{1}{6}[1 &+ 2(f_1^2(t) + h_3^2(t) + k_3^2(t)) - 4f_1(t)k_3(t)\cos(\omega_1+\omega_3)t \\ &+4f_1(t)h_3(t)\cos(\omega_1+\omega_2)t - 4h_3(t)k_3(t)\cos(\omega_2-\omega_3)t].\end{aligned} \tag{4.7b}$$

Note that in all the above calculations we have used the identities which were given by equations (2.7) and (2.8). In figures 8(*a*) and (*b*) we have plotted the quadrature variances $\overline{\Delta X_1^2}$ and $\overline{\Delta Y_1^2}$, against time for two different cases. The first one is the case in which we take $\lambda_3^2 > \lambda_1^2 + \lambda_2^2$, while in the second case we take $\lambda_3^2 < \lambda_1^2 + \lambda_2^2$. For $t > 0$ we can easily observe that the squeezing starts in the second quadrature $\overline{\Delta Y_1^2}$ for all cases, however, we also observe exchanging between the quadrature variances $\overline{\Delta X_1^2}$ and $\overline{\Delta Y_1^2}$. This phenomena is expected as a result of the existence of the oscillating terms in each quadrature. Thus, we may conclude that as a result of the correlation between the modes in the definition of the quadrature operators, X_1 and Y_1, we managed to observe the squeezing in our system. The quadratures' behaviours for the other two cases, equations (4.5) and (4.7), are similar to that given in the first case.

As we stated above, there is no squeezing in the quadrature variances $\overline{\Delta X^2}$ and $\overline{\Delta Y^2}$, where

$$X = \frac{a_1^\dagger + a_1}{2} \qquad Y = \frac{a_1 - a_1^\dagger}{\mathrm{i}\sqrt{2}}.$$

However, if we examine these quadrature variances taken into consideration, the even coherent state to be our initial state, then the phenomena of squeezing can be observed [30, 31]. To see that, let us define the even coherent state for three modes, thus

$$|\eta\rangle = \Pi_{i=1}^3 N_{\alpha_i} \sum_{j=1}^{2} |\alpha_i \mathrm{e}^{\mathrm{i}\phi_j}\rangle \qquad \phi_{1,2} = \pi, 2\pi \tag{4.8a}$$

and

$$N_{\alpha_i} = \tfrac{1}{2}\exp(\tfrac{1}{2}|\alpha_i|^2)\sqrt{\mathrm{sech}|\alpha_i|^2}. \tag{4.8b}$$

From equations (2.7*a*) and (4.8) we find

$$\begin{aligned}\overline{\Delta X^2} = f_1^2(t)[1 &+ |\alpha_1|^2(\cos 2(\omega_1 t + \delta_1) + \tanh|\alpha_1|^2)] \\ &+ f_2^2(t)|\alpha_2|^2[\tanh|\alpha_2|^2 + \cos 2(\omega_1 t - \delta_2)] \\ &+ f_3^2(t)|\alpha_3|^2[\tanh|\alpha_3|^2 + \cos 2(\omega_1 t - \delta_3)]\end{aligned} \tag{4.9a}$$

and

$$\begin{aligned}\overline{\Delta Y^2} = f_1^2(t)[1 &+ |\alpha_1|^2(\tanh|\alpha_1^2| - \cos 2(\omega_1 t + \delta_1)] \\ &+ f_2^2(t)|\alpha_2|^2[\tanh|\alpha_2|^2 - \cos 2(\omega_1 t - \delta_2)] \\ &+ f_3^2(t)|\alpha_3|^2[\tanh|\alpha_3|^2 - \cos 2(\omega_1 t - \delta_3)].\end{aligned} \tag{4.9b}$$

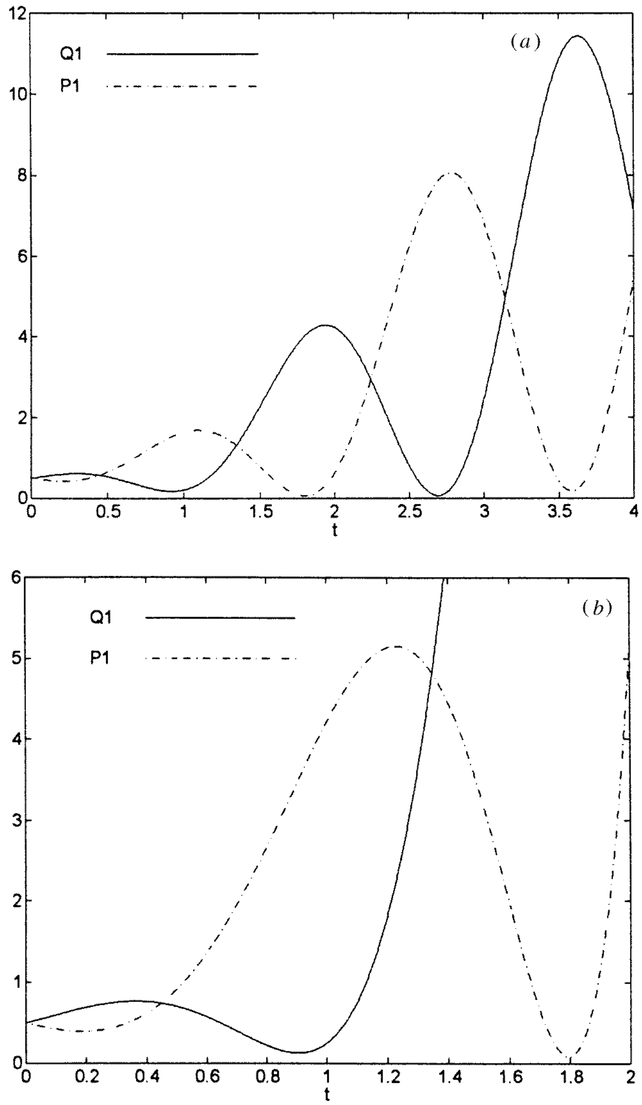

Figure 8. (*a*) The quadrature variances $\overline{\Delta X_1}^2 = Q_1$ and $\overline{\Delta Y_1}^2 = P_1$ against time with $\omega_i = (2, 1.5, 1)$ and $\lambda_i = (0.5, 0.4, 0.9)$. (*b*) As in (*a*) but with $\lambda_i = (0.9, 0.7, 0.4)$.

In figures 9(*a*) and (*b*) we have plotted the quadrature variances $\overline{\Delta X}^2$ and $\overline{\Delta Y}^2$ against time in two cases; (i) when $\lambda_3^2 > \lambda_1^2 + \lambda_2^2$, and (ii) when $\lambda_3^2 < \lambda_1^2 + \lambda_2^2$. For the even coherent state we find that for a fixed value of the photon numbers, the reduction of fluctuations occur in $\overline{\Delta Y}^2$, while the fluctuations in $\overline{\Delta X}^2$ are enhanced. From the above it follows that quadrature squeezing can emerge as a consequence of the quantum interference between coherent states.

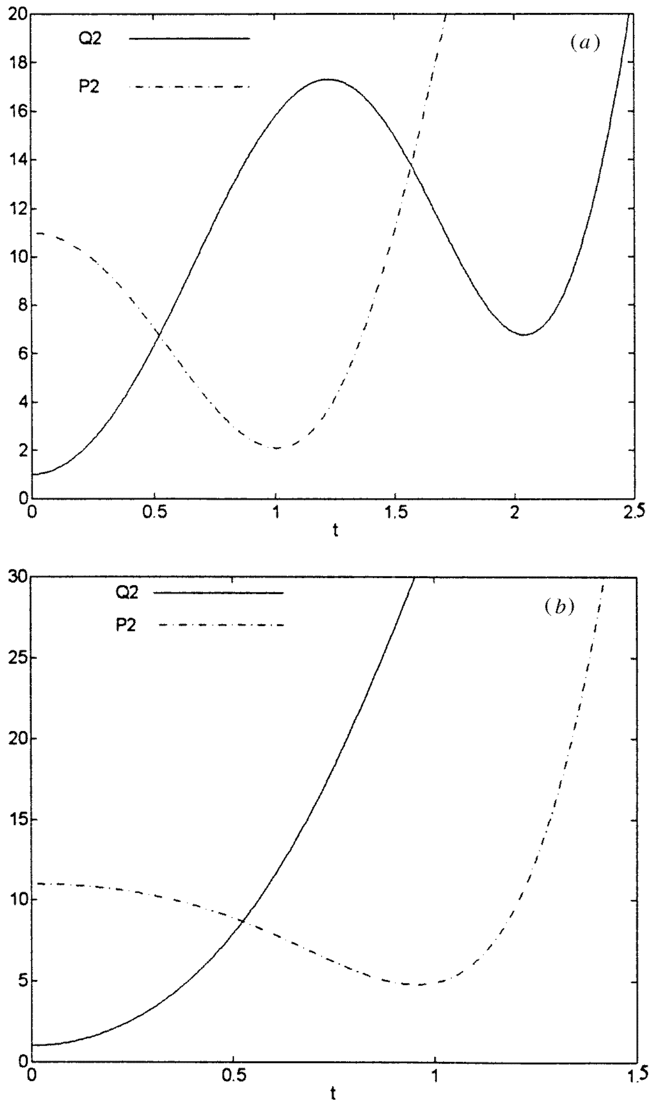

Figure 9. (a) The quadrature variances $\overline{\Delta X}^2 = Q_2$ and $\overline{\Delta Y}^2 = P_2$ for the even-coherent state against time with $\omega_1 = 1.5$, $|\alpha_i|^2 = (5, 1, 1)$, $\lambda_i = (0.5, 0.4, 0.9)$ and $\delta_i = (\pi/2, \pi/2, \pi)$. ($b$) As in ($a$) but with $\lambda_i = (0.9, 0.7, 0.5)$.

5. The quasiprobability functions

The representation of quantum fields in phase space in terms of quasiprobabilities is widely used in the field of quantum optics, with particular emphasis on the Glauber–Sudershan P-representation, the W-Wigner and Q-functions. In fact these functions are important for providing insight into the non-classical features of the radiation field besides the statistical description of a microscopic system. To present a general form for the quasiprobability distribution function for different forms of phased orthogonal states, we have to calculate the function [32, 33]

$$F(\alpha_1,\alpha_2,\alpha_3,s)=\frac{1}{\pi^6}\int_{-\infty}^{\infty}C(\xi_1,\xi_2,\xi_3,s)\prod_{i=1}^{3}\exp(\alpha_i\xi_i^*-\alpha_i^*\xi_i)\,\mathrm{d}^2\xi_i \tag{5.1}$$

where $C(\xi_i, s)$ is the s-ordered generalized characteristic function given by

$$C(\xi_1,\xi_2,\xi_3,s)=\mathrm{Tr}\left[\hat\rho(0)\prod_{i=1}^{3}\exp\left(\xi_i a_i^\dagger-\xi_i^*a_i+\frac{s}{2}|\xi_i|^2\right)\right] \tag{5.2}$$

where $\hat\rho(0)=|\alpha\rangle\langle\alpha|$ is the density matrix operator, and s is a parameter that defines the relevant quasiprobability distribution functions. For $s = 1$ we obtain the Glauber–Sudershan P-function, for $s = 0$ we have the Wigner function, while the Q-function is obtained for $s = -1$. It is worth pointing out that as a result of non-classical character of the mixing modes, the P-representation function is highly singular, and then the consideration of this function is meaningless. The characteristic function (5.2) is calculated and has the following expression

$$\begin{aligned}
C(\xi_1,\xi_2,\xi_3,s) = {} & \exp[-\tfrac{1}{2}(2f_1^2(t)-1-s)|\xi_1|^2]\\
& \times\exp[-\tfrac{1}{2}(2h_3^2(t)+1-s)|\xi_2|^2-\tfrac{1}{2}(2k_3^2(t)+1-s)|\xi_3|^2]\\
& \times\exp[-k_3(t)h_3(t)(\xi_2\xi_3^*\mathrm{e}^{\mathrm{i}(\omega_2-\omega_3)t}+\xi_2^*\xi_3\mathrm{e}^{-\mathrm{i}(\omega_2-\omega_3)t})]\\
& \times\exp[f_1(t)h_3(t)(\xi_1\xi_2\mathrm{e}^{\mathrm{i}(\omega_1+\omega_2)t}+\xi_1^*\xi_2^*\mathrm{e}^{-\mathrm{i}(\omega_1+\omega_2)t})]\\
& \times\exp[f_1(t)k_3(t)(\xi_1\xi_3\mathrm{e}^{\mathrm{i}(\omega_1+\omega_3)t}+\xi_1^*\xi_3^*\mathrm{e}^{-\mathrm{i}(\omega_1+\omega_3)t})]\\
& \times\exp\sum_{i=1}^{3}(\xi_i\bar\alpha_i^*(t)-\xi_i^*\bar\alpha_i(t))
\end{aligned} \tag{5.3}$$

where $\bar\alpha_i(t)$ is the mean value of the operators $a_i(t)$, $i = 1, 2, 3$ with respect to the coherent state given by equation (2.9).

By inserting equation (5.3) into equation (5.1) and performing the integral for $s = 0$, we find that the Wigner function takes the following form

$$\begin{aligned}
W(\alpha_1,\alpha_2,\alpha_3,t) = {} & \frac{4}{\pi^3}A(t)[A(t)-(h_3(t)\cos\phi-k_3(t)\sin\phi)^2]^{-1}\\
& \times[A(t)-(k_3(t)\cos\phi+h_3(t)\sin\phi)^2]^{-1}\exp\left(-\frac{|J_1|^2}{A(t)}\right)\\
& \times\exp\Bigg(-\frac{2}{A(t)}\{|[(f_1(t)h_3(t)J_1(t)-A(t)J_3^*(t)]\cos\phi\\
& +[f_1(t)h_3(t)J_1(t)-A(t)J_2^*(t)]\sin\phi|^2\}\\
& \times\{[A(t)-(k_3(t)\cos\phi+h_3(t)\sin\phi)^2]\}^{-1}\Bigg)\\
& \times\exp\Bigg(-\frac{2}{A(t)}\{|[(f_1(t)h_3(t)J_1(t)-A(t)J_2^*(t)]\cos\phi\\
& -[f_1(t)h_3(t)J_1(t)-A(t)J_3^*(t)]\sin\phi|^2\}\\
& \times\{[A(t)-(h_3(t)\cos\phi-k_3(t)\sin\phi)^2]\}^{-1}\Bigg)
\end{aligned} \tag{5.4}$$

where

$$\phi=\frac{1}{2}\tan^{-1}\left(\frac{k_3(t)h_3(t)}{k_3^2(t)-h_3^2(t)}\right) \tag{5.5}$$

$A(t) = (f_1^2(t) - \frac{1}{2})$ and $J_j(t) = (\bar{\alpha}_j(t) - \alpha_j)\exp(\mathrm{i}\omega_j t)$ while $\bar{\alpha}_j(t)$ is the mean value of the operators a_j, $j = 1, 2, 3$ with respect to the coherent state given by equation (2.7). The Q-function can also be found when $s = -1$ and the calculation gives

$$Q(\alpha_1, \alpha_2, \alpha_3, t) = \frac{f_1^{-2}(t)}{\pi^3} \exp\left(-\frac{(1 + 2h_3^2(t))}{f_1^2(t)}|J_1|^2\right) \exp\left[-(|J_2|^2 + |J_3|^2) + \frac{h_3(t)}{f_1(t)}[J_1(t)(J_2(t) + J_3(t)) + J_1^*(t)(J_2^*(t) + J_3^*(t))]\right]. \tag{5.6}$$

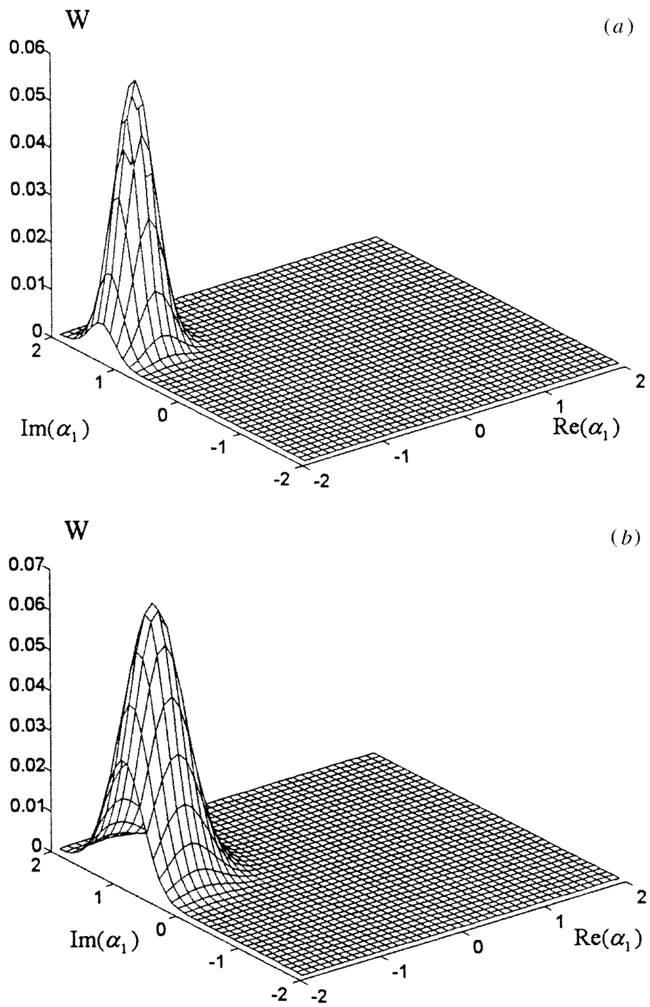

Figure 10. (*a*) The Wigner function against $\mathrm{Re}\,\alpha_1$ and $\mathrm{Im}\,\alpha_1$ with $t = \pi/3$, $\omega_i = (1.75, 1.5, 1)$, $|\alpha_i|^2 = (1, 1, 1)$, $\lambda_i = (0.9, 0.7, 0.5)$ and $\delta_i = (\pi/2, \pi/2, \pi)$. (*b*) As in (*a*) but with $\lambda_i = (0.5, 0.4, 0.9)$.

In figures 10(*a*) and (*b*) we have plotted the Wigner functions $W(\alpha_1, t)$ against $\mathrm{Re}\,\alpha_1$ and $\mathrm{Im}\,\alpha_1$ in two different cases; the first where $\lambda_1^2 + \lambda_2^2 > \lambda_3^2$, and the second when $\lambda_1^2 + \lambda_2^2 < \lambda_3^2$. The shape of the function is Gaussian for both cases, however, the peak in general is sharper in the case where $\lambda_1^2 + \lambda_2^2 > \lambda_3^2$, than that for the case when $\lambda_1^2 + \lambda_2^2 < \lambda_3^2$.

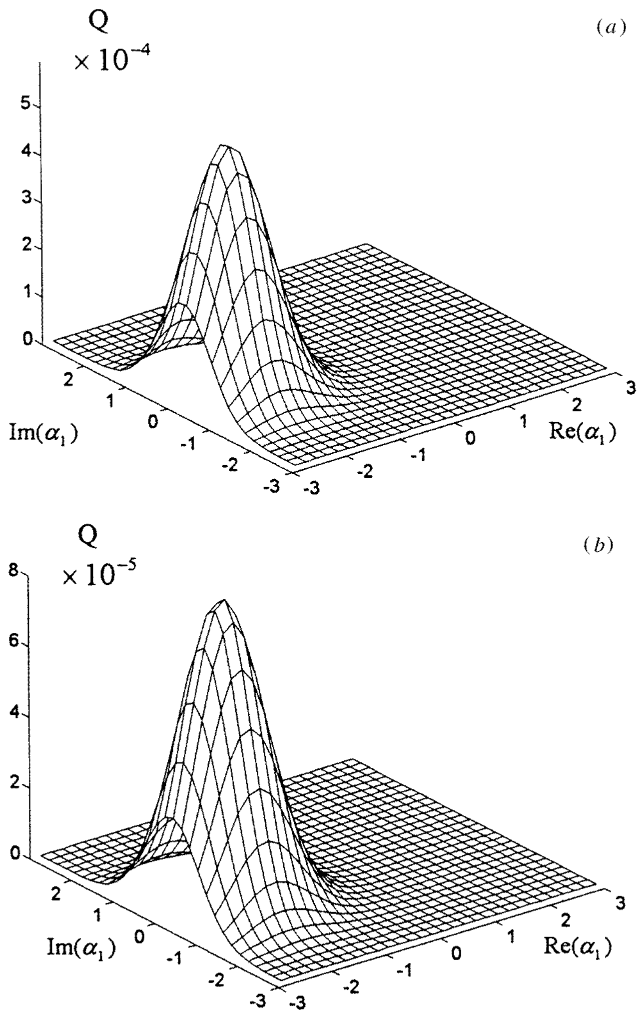

Figure 11. (a) The Q-function against $\mathrm{Re}\,\alpha_1$ and $\mathrm{Im}\,\alpha_1$ with the same value of the parameters in figure 10(a) for Wigner function but with $t = \pi/4$. (b) As in (a) but with $\lambda_i = (0.5, 0.4, 0.9)$.

This of course is due to the existence of the hyperbolic function in the expression of the Wigner function. In the meantime we can easily realize that for some values of t stretching occurs in the function; this is due to the non-classical character of the system, which is actually a result of the correlation between the modes. A similar behaviour is found for $W(\alpha_2, t)$ and $W(\alpha_3, t)$, but the value of these two functions are smaller than the value for $W(\alpha_1, t)$. The Q-function has been plotted in figures 11(a) and (b); the analysis for Wigner function would be applied for the Q-function. However, there is a slight difference between the two functions, for example we can see that the Wigner function is sharper than the Q-function, but we can also see that the stretching occurring in the Q-function is more pronounced than that which occurs in the Wigner function. This can be realized for the case in which $\lambda_1^2 + \lambda_2^2 < \lambda_3^2$, where we have plotted the Q-function against $\mathrm{Re}\,\alpha_1$ and $\mathrm{Im}\,\alpha_1$, see figures 10(b) and 11(b). In contrast we find that the stretching in the Wigner function is more pronounced than that in the Q-function for the other two cases, this can be seen if

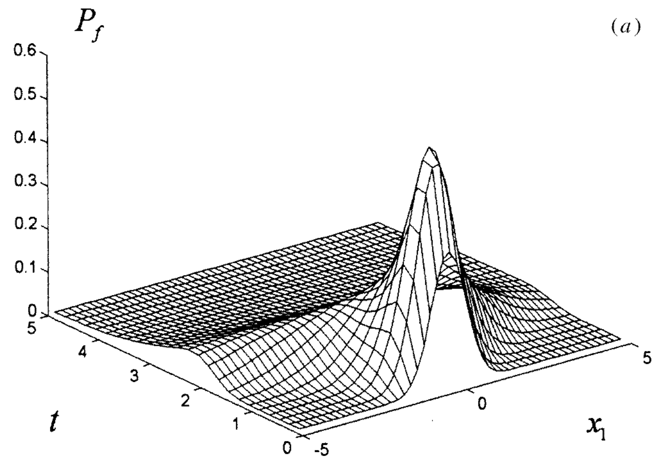

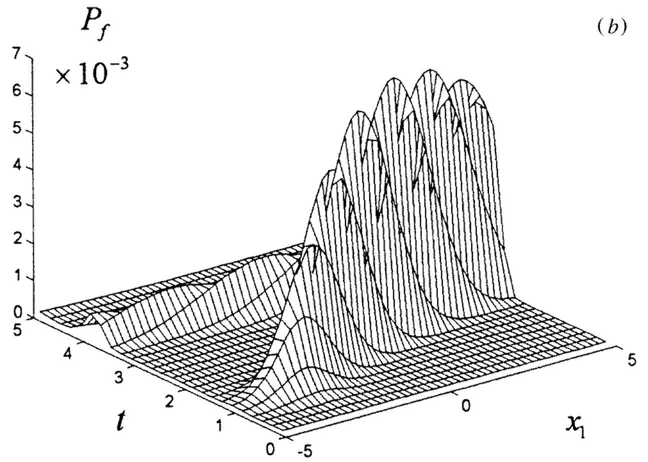

Figure 12. (*a*) The distribution function $P_f(x_1, t)$ against time and the axis x_1, with $\omega_1 = 1.75$, $\lambda_i = (0.9, 0.7, 0.5)$, $\delta_i = (\pi/2, \pi/2, \pi/2)$ and $|\alpha_i|^2 = (1, 1, 1)$. (*b*) As in (*a*) but with $\lambda_i = (0.5, 0.4, 0.9)$, and $|\alpha_i|^2 = (10, 1, 1)$.

we plot the Wigner function against $\mathrm{Re}\,\alpha_i$ and $\mathrm{Im}\,\alpha_i$, $i = 2, 3$. Finally we may refer to the effect of the photon numbers as well as the time on both of the Wigner function and the Q-function, where we have realized as we increase the value of the photon numbers, then the height of the peak is always decreasing, while we find that the stretching is decreasing as the time increases.

Now let us turn our attention to considering the distribution function $P_f(x_1, t)$ associated with the field quadrature component $x_i = \mathrm{Re}\,\alpha_i$ for one single mode a_1, (say) where

$$P_f(x_1, t) = \int_{-\infty}^{\infty} W(\alpha_1, t)\, \mathrm{dIm}\,\alpha_1 \tag{5.7}$$

$W(\alpha_1, t)$ is the Wigner function given from the equation

$$W(\alpha_1, t) = \frac{1}{\pi^2}\int_{-\infty}^{\infty} \exp[-(f_1^2(t) - \tfrac{1}{2})|\xi_1|^2 + \bar{\alpha}_1^*(t)\xi_1 - \bar{\alpha}_1(t)\xi_1^*]\, \mathrm{d}^2\xi_1. \tag{5.8}$$

The exponential function in the above integral represents the characteristic function for one

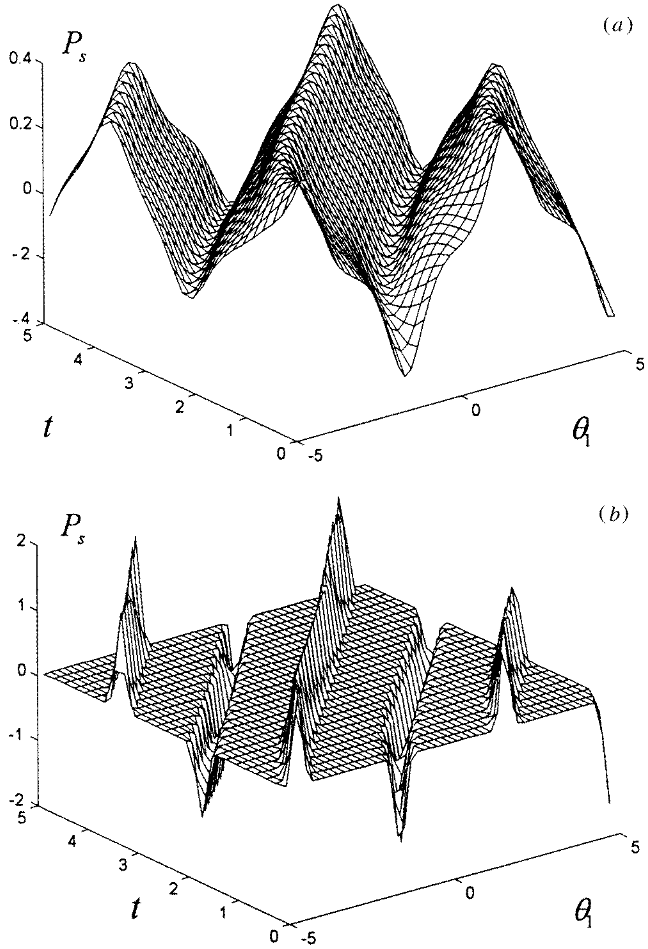

Figure 13. (a) The phase-space distribution function against time and the phase with $\omega_1 = 1.75$, $\lambda_i = (0.5, 0.4, 0.9)$, $|\alpha_i|^2 = (1, 1, 1)$ and $\delta_i = (\pi/2, \pi/4, \pi/4)$. ($b$) As in ($a$) but with $|\alpha_i|^2 = (20, 20, 1)$.

single mode a_1. Evaluating the integral in equation (5.8) leads to

$$W(\alpha_1, t) = \frac{(f_1^2(t) - \frac{1}{2})^{-1}}{\pi} \exp\left(-\frac{|\bar{\alpha}_1(t) - \alpha_1|^2}{(f_1^2(t) - \frac{1}{2})}\right). \tag{5.9}$$

The distribution function $P_f(x_1, t)$ is ready to be calculated if one uses equation (5.7) together with equation (5.9); this gives

$$P_f(x_1, t) = [\pi(f_1^2(t) - \tfrac{1}{2})]^{-\frac{1}{2}} \exp\left[-\frac{|\bar{\alpha}_1(t)|^2}{(f_1^2(t) - \frac{1}{2})}\right] \exp\left[-\frac{(x_1 - \mathrm{Re}\,\bar{\alpha}_1(t))^2}{(f_1^2(t) - \frac{1}{2})}\right]. \tag{5.10}$$

In figures 12(a) and (b) we have plotted the distribution function $P_f(x, t)$ against both x_1 and t. The shape of the function is Gaussian, and the value of it changes as the time varies. In the meantime we have realized that as we increase the value of the photon numbers, then the value of the distribution function decreases, this means that the maximum value of this function will be at $\bar{n}_i = 0$.

The phase-space distribution function can also be found when we calculate the integral

$$P_s(\theta_1, t) = \int_0^\infty W(\alpha_1, t)|\alpha_1|\, \mathrm{d}|\alpha_1| \tag{5.11}$$

where $\alpha_1 = |\alpha_1|\mathrm{e}^{-\mathrm{i}\theta_1}$. By inserting equation (5.9) into equation (5.11), and after some minor algebra we have

$$P_s(\theta_1, t) = \left[\frac{1}{2\pi} + \frac{1}{4}\frac{(\bar{\alpha}_1\mathrm{e}^{\mathrm{i}\theta_1} + \bar{\alpha}_1^*\mathrm{e}^{-\mathrm{i}\theta_1})}{\sqrt{\pi(f_1^2(t) - \frac{1}{2})}} \times \exp\frac{(\bar{\alpha}_1\mathrm{e}^{\mathrm{i}\theta_1} + \bar{\alpha}_1^*\mathrm{e}^{-\mathrm{i}\theta_1})^2}{4(f_1^2(t) - \frac{1}{2})}\right] \exp\left[-\frac{|\bar{\alpha}_1|^2}{(f_1^2 - \frac{1}{2})}\right] \tag{5.12}$$

where $\bar{\alpha}_1(t)$ is the mean value of the operator $a_1(t)$ given by equation (2.9a) with respect to the coherent state.

The behaviour of the above equation can be seen in figures 13(a) and (b), where we have plotted the phase-space distribution function against both time and phase. We find that the value of the function is always increasing as we increase the value of the photon numbers, so that it would take positive or negative values larger than that when we take small number of photons.

6. Conclusion

In this paper we have considered the problem of three modes time-dependent coupled oscillators. The model is considered to describe mutual interaction between phonon and Stokes, phonon and anti-Stokes, and Stokes and anti-Stokes. The Hamiltonian model has been derived in the light of the quantization of the cavity modes, and is connected to the directional coupler system. The solution in the Heisenberg picture is obtained and used to calculate the photon numbers in both number state and coherent state. The examination of bunching and antibunching are considered where we found that the system shows bunching and antibunching in the case of number state, while it shows only bunching in the case of coherent state. We also found that for one single mode the system does not exhibit squeezing, while for mixing mode the squeezing phenomena is observed. The quasiprobability distribution functions (W-Wigner and Q-functions), besides the phase-space distribution, has also been considered and numerical investigations were carried out.

Acknowledgments

MSA would like to thank Professor J Pẽrina for useful discussions. SA-H thanks King Fahd University of Petroleum and Minerals for financial support.

References

[1] Louisell W H, Yariv A and Siegman A E 1961 *Phys. Rev.* **124** 1646
[2] Louisell W H 1960 *Coupled Mode and Parametric Electronics* (New York: Wiley)
[3] Tucker J and Walls D F 1969 *Phys. Rev.* **178** 2036
[4] Mishkin E A and Walls D F 1969 *Phys. Rev.* **185** 1618
[5] Walls D F and Barakat R 1970 *Phys. Rev.* **1** 446
[6] Georgiades N Ph, Polzik E S, Edamatsu K and Kimble H J 1995 *Phys. Rev. Lett.* **75** 3426
[7] Engelbrecht C A (ed) 1982 *Lecture Notes in Physics* (Berlin: Springer) p 103
[8] Pẽrine J 1991 *Quantum Statistics of Linear and Nonlinear Optical Phenomena* (Dordrecht: Kluwer)
[9] Loudon R 1983 *The Quantum Theory of Light* (Oxford: Clarendon)

[10] Agrawal G P and Mehta C L 1974 *J. Phys. A: Math. Gen.* **7** 607
[11] Bandilla A, Drobny G and Jex I 1996 *Phys. Rev.* A **53** 507
[12] Shumovsky A S and Tanatar B 1993 *Phys. Rev.* A **48** 4735
[13] Carusotto S 1989 *Phys. Rev.* A **40** 1848
[14] Louisell W H 1973 *Quantum Statistical Properties of Radiation* (New York: Wiley)
[15] Garrett G A, Rojo A G, Sood A K, Whitaker J F and Merlin R 1997 *Science* **275** 1638
[16] Abdalla M S 1987 *Phys. Rev.* A **35** 4160
[17] Abdalla M S 1990 *Phys. Rev.* A **41** 3775
[18] Abdalla M S 1996 *J. Phys. A: Math. Gen.* **29** 1997
[19] Yurke B 1985 *J. Opt. Soc. Am.* B **2 732**
[20] Abdalla M S 1994 *Physica* **202A** 301
[21] Abdalla M S 1994 *Nuovo Cimento* B **109** 443
[22] Abdalla M S 1997 *Acta Phys. Slovaca* **47** 353 and references therein
[23] Pieczonkova A 1982 *Opt. Acta* **29** 1509
[24] Colegrave R K and Croxson P 1991 *J. Math. Phys.* **32** 3361
[25] Barnett S M and Knight P L 1987 *J. Mod. Opt.* **34** 841
[26] Abdalla M S and Bashir M A 1998 *Quantum Semiclass. Opt.* **10** 415
[27] Adam P, Janszky J, Petak A, Sibilia C and Bertolotti M 1995 *Acta Phys. Slovaca* **45** 331
[28] Janszky J, Sibilia C, Bertolotti M, Adam P and Petak A 1995 *Quantum Opt.* **7** 509
see also Perina J and Perina J Jr 1995 *Quantum Opt.* **7** 541
[29] Special issue of 1987 *J. Mod. Opt.* **34**
Special issue of 1987 *J. Opt. Soc. Am.* B **4**
[30] Dodonov V V, Malkin I A and Man'ko V I 1974 *Physica* **72** 597
[31] Bužek V and Knight P L 1991 *Opt. Commun.* **81** 331
[32] Glauber R J 1963 *Phys. Rev.* **131** 2766
[33] Mollow B R 1967 *Phys. Rev.* **162** 1256